A computational study of HCCI engine with external mixture formation technique.

Conference Paper · November 2014

1 author:

T.Karthikeya Sharma
National Institute of Technology, Andhra Pradesh

Proceedings of the ASME 2014 International Mechanical Engineering Congress & Exposition
IMECE2014
November 14-20, 2014, Montreal, Quebec, Canada

IMECE2014-37211

A COMPUTATIONAL STUDY OF HCCI ENGINE WITH EXTERNAL MIXTURE FORMATION TECHNIQUE

T.Karthikeya Sharma
Research Scholar
Department of Mechanical Engineering
NIT Warangal-506004(A.P)-India
karthikeya.sharma3@gmail.com

G.Amba Prasad Rao
Professor in MED
Department of Mechanical Engineering
NIT Warangal-506004(A.P)-India
gap@nitw.ac.in

Madhu Murthy Kotha
Professor in MED
Department of Mechanical Engineering,
NIT Warangal-506004(A.P)-India
madhu@nitw.ac.in

ABSTRACT

HCCI combustion is gaining increased attention amongst the research community to make it viable in both diesel and gasoline engines. Of late, technique of External mixture formation is being adopted to avoid the problems associated with the early injection and late injections of the direct injected diesel HCCI engine. This paper reports the numerical studies on the effect of External mixture formation using three-zone extended coherent flame (ECFM-3Z) CFD model of the STAR - CD package. Firstly, the results obtained through package were validated with the results available in the literature. Trade-off between HC, CO and NOx was clearly observed through simulation. The simulation results revealed decrease in in-cylinder pressures and NO_x emissions with increase in EGR concentration. There is an under prediction of NO_x emissions when compared with the experimental results. However, a significant reduction in NO_x emissions was observed with external mixture formation, usage compared to direct diesel injection. In case of HC and CO emissions increasing trend was observed with increase in EGR concentration. Increase in HC and CO emissions was observed with external mixture formation when compared with a direct diesel injection. Also, reduction in turbulent kinetic energy and velocity magnitude levels were observed with increase in EGR concentration. Improved piston work is resulted at lower EGR concentrations. Studies revealed that for a given combustion bowl geometry, It is concluded that external mixture formation technique could be adopted to achieve HCCI combustion.

Key words: HCCI; external mixture formation; EGR; ECFM-3Z.

INTRODUCTION

IC Engines have become indispensable prime movers over the past one and half century. Though the performance of conventional SI and CI engines is satisfactory, SI engine suffers from poor part load efficiency and high CO emissions. The CI engine yields high particulate and NOx emissions. These effects may be attributed to their conventional combustion process. Of late, a hybrid combustion process called Homogeneous charge compression ignition (HCCI) equipped with advanced low-temperature combustion technology is gaining attention by researchers. In principle, HCCI involves the volumetric auto combustion of a premixed fuel, air, and diluents at low to moderate temperatures and at high compression ratios. Epping (2008), The other associated advantages with HCCI mode of combustion have been well documented and presented as a potentially promising combustion mode for internal combustion engines.

Also to arrive at the optimum design of engine multidimensional modelling through CFD modelling has also gained a lot of interest among researchers with precise prediction of engine in-cylinder flow conditions. Especially CFD simulation of engine is aimed at understanding turbulent mixing between fuel and air, the ignition and combustion chemistry, knock occurrence, formation and destruction of pollutants like NOx and soot, the influence of exhaust gas recirculation (EGR) on the emissions, power output and efficiency.

EXTERNAL MIXTURE FORMATION

Thring et al., (1989) achieved HCCI conditions by varying the intake temperature and EGR fraction over a range of equivalence ratios. Yanagihara et al., (2001) achieved HCCI by using a combination of early injection and late injection and studied the emissions. Lei shi et al., (2006) have utilized the thermal energy of trapped exhaust gases to vaporize the fuel. Diesel was directly injected into the cylinder near the intake TDC and valve overlap was adjusted to obtain a high internal exhaust gas recirculation. The effect of the engine load, speed, inlet temperature, external and internal EGR on HCCI combustion and emissions was studied. Simescu et al., (2003) conducted an experimental investigation of Premixed Charge Compression Ignition (PCCI) - DI combustion coupled with cooled and uncooled EGR in a Heavy Duty (HD) diesel engine. Shawn Midlam-Mohler et al., (2003) have developed an atomizer for external mixture preparation and the authors have investigated the effect of un-cooled EGR, boost pressure, air–fuel ratio, intake air temperature, swirl and engine speed on HCCI combustion.

From the previous research works, it is noticed that, early injection, late injection and port fuel injection systems like Air assisted port injection with DI system (PCCI-DI) were used. In addition to that high levels of EGR and reduced compression ratio were demonstrated for simultaneous and substantial reduction of NOx and smoke emissions. In the above detailed methods the mixture was partially homogeneous. Hence the present system was developed to prepare a homogeneous mixture. This paper reports the results of detailed examination of the basic characteristics of HCCI combustion in which a different method of preparing a homogeneous mixture of fuel and air (usually by early injection, late injection and air assisted port fuel injection) was demonstrated by using a device called fuel vaporizer and its effect on engine emissions, performance and combustion are investigated with various EGR proportions and without modifying the compression ratio of an engine. The results show that through this approach simultaneous and substantial reduction of NOx and smoke emission can be achieved.

COMBUSTION MODEL

Many commercial CFD packages like Open FOAM, Ricardo Wave, GT Power, AVL FIRE are available to simulate the combustion process in IC engines. In the present work “es-ice” of STAR –CD is used for the analysis. The different combustion models which are well developed for predicting engine processes are Transient Interactive Flamelets (TIF) model, Digital Analysis of Reaction System – Transient Interactive Flamelets model (DARS-TIF), G –equation model, Extended Coherent Flame Combustion Model -3 Zones Duclos et al., (1999), Colin and Benkenida (2004) and the Equilibrium-Limited ECFM (ECFM-CLEH) Ravet et al.,(2008), Subramanian et al., (2007), Each model has its own limitations and is suitable for a specific set of problems. Generally speaking; ECFM-3Z and ECFM-CLEH can be used for all types of combustion regime, whereas ECFM-3Z is mostly suitable for homogeneous turbulent premixed combustion with spark ignition and Compression Ignition. Various combustion models applicabilities are shown in Table 1.

Table 1: Combustion Models Capabilities

Model	Applicability
G-Equation	Partially Premixed S.I& C.I
DARS-TIF	Compression Ignition
ECFM	Non-Homogeneous Premixed S.I.
ECFM- 3Z	Premixed and Non Premixed S.I And C.I

Owing to its wide applicability, ECFM- 3Z has been used for predicting engine performance in both HCCI and conventional mode of operation.

METHODOLOGY

A single cylinder direct injection, spherical piston bowl, CI engine with the specifications given in Table 2 has been taken for the analysis. A CFD package STAR-CD is used for the analysis to study the in-cylinder flame distribution, heat release rates, in-cylinder pressures and temperatures, CO and NO emissions were studied in CI engine in conventional and in HCCI Mode. The engine specifications considered for the analysis are shown in Table 2.

The analysis was done from the second cycle after the engine has started. Table 3 shows the starting and stopping crank angles between which the analysis is carried out.

Table 2. Engine Specifications.

Specification	Value
Bore	87.5 mm
Stroke	110 mm
Connecting Rod Length(L)	233 mm
Equivalence ratio	0.5
Compression Ratio	17.5:1
Number of Cylinders	1

Table 3. Operating conditions of the analysis.

Specification	Value
Start crank angle	680
Stop crank angle	820
Engine RPM	1500

CFD MODEL SET- UP

The piston bowl shape and 3D mesh of the piston bowl sector is shown in Fig 1. The computational mesh consists of $0.312\text{x}10^6$ cells. The entire mesh consists of cylinder and 1/8th of the piston bowl created in Hypermesh—a mesh generation utility and is imported into STAR-CD for solutions. A spline has been developed based on the imported model; 2D template was cut by the spline to cut the 3D mesh with 60 radial cells, 160 axial cells, 5 top dead center layers and 40 axial block cells.

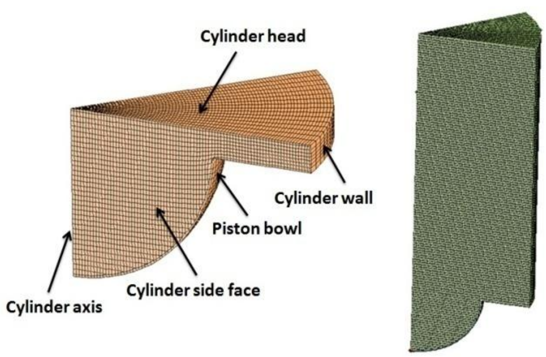

Figure 1. Schematic representation of piston bowl shape and the 3D mesh prepared

The energy efficiency of the engine is analysed by gross indicated work per cycle (*W)* calculated from the cylinder pressure and piston displacement using Eq. (1):

$$W(Nm) = \frac{\pi a B_2}{8}\int_{\theta_1}^{\theta_2} p(\theta)\left[2\sin(\theta) + \frac{a\sin(2\theta)}{\sqrt{l^2 - a^2\sin^2(\theta)}}\right]d\theta \qquad (1)$$

where *a*, *l*, and *B* are the crank radius, connecting rod length and cylinder bore, respectively, and θ_1 and θ_2 are the beginning and the end of the valve-closing period.

The indicated power per cylinder (*P*) is related to the indicated work per cycle by using Eq.(2):

$$P(kW) = \frac{WN}{60000\, n_R} \qquad (2)$$

where n_R=2 is the number of crank revolutions for each power stroke per cylinder and *N* is the engine speed (rpm). The indicated specific fuel consumption (ISFC) is shown in Eq.(3):

$$\mathrm{ISFC(g / kWh)} = \frac{30\, \mathrm{m_{fuel}}\ \mathrm{N}}{\mathrm{P}} \qquad (3)$$

In Eq. (1), the power and ISFC analyses can be viewed as being only qualitative rather than quantitative in this study.

MODELING STRATEGY

The STAR-CD used in the present study has integrated several sub models such as turbulence, fuel spray and atomization, wall function, ignition, combustion, NOx, and soot models for various types of combustion modes in CI as well as SI engine computations. The turbulence is modelled using I-L model. The Combustion is modeled using ECFM-3Z. As far as fluid properties are concerned, ideal gas law and temperature dependent constant pressure specific heat (C_p) are chosen.

Spray injection and atomization model

In conventional CI mode, spray and atomization are modelled using Huh's model based on Huh et al.,(1991), Bai et al.,(1995). Huh's model considers the two most important mechanisms in spray atomization: gas inertia and the internal turbulence stresses generated in the nozzle. The agitation of jet takes place because of turbulence generated in the nozzle when it exits the hole. Surface wave growth takes place once the agitation of jet reaches a certain limit leading to droplet formation.

The secondary break –up of the droplets is modeled by considering Reitz - Diwakar model based on Reitz, Diwakar (1986,1987). The Reitz - Diwakar model incorporates the droplet break-up due to non-uniform pressure surrounding the droplet (bag break-up) and the other is because of continuous phase (stripping break-up). The occurrence of these regimes is dependent on the magnitude of the droplet incidence Weber number (We*d*) and the dimensionless droplet diameter *d** is shown in Eq. (4):

$$We_d = \frac{\rho_d D_d V_{d,n}^2}{\sigma} \qquad (4)$$

Where 'n' is the unit normal to the wall, '$V_{d,n}$' the normal component of droplet velocity relative to the wall, 'σ' the surface tension coefficient.

For HCCI combustion mode the premixed reaction mechanism is adopted for the homogeneous fuel air mixture formation.

Auto ignition model

Ignition delay is computed to establish the ignition occurrence time, instead of the pre-ignition kinetics.

The auto-ignition delay τ_d is calculated based on semi empirical correlations as shown in Eq.(5):

$$\tau_d = 1.051\text{x}10^{-8}[F]^{0.05}[O_2]^{-0.53}\rho^{0.13}\, e^{\,5914/T\mu}[47/CN] \qquad (5)$$

where CN the cetane number (max=60). An ignition progress variable function is defined to track the development of the reactions prior to autoignition as shown in Eq.(6):

$$(\,dY_{igi}\,)/(dt) \quad = Y_{Tf}F(\tau_d) \qquad (6)$$

For HCCI Combustion Mode a double delay autoignition model is used as the autoignition in HCCI mode is controlled by the effect of cool flames. In cool flame regime, the rise in temperature is less and the reaction rates get slowed down. After the second delay the reaction rates increases leading to main autoignition.

Double delay autoignition considers two delay times and two ignition progress variables. The delay times are not empirical correlations but are obtained from pre computed tables, which can also provide the information about the maximum fuel burnt at each autoignition step.

Combustion model

A Three Zone Extended Coherent Flame Combustion Model (EFCM -3Z) is used for the analysis. Premixed charge with auto ignition has been considered for the start of combustion.

In HCCI engine the air fuel mixture enters the cylinder like in SI engines, combustion occurs by compression Ignition like in CI engines. Fig 2.depicts the schematic representation of the three zones of the ECFM- 3Z model.

This model is capable of simulating the complex mechanisms like turbulent mixing, flame propagation, diffusion combustion and pollutant emission that characterize modern IC engines.

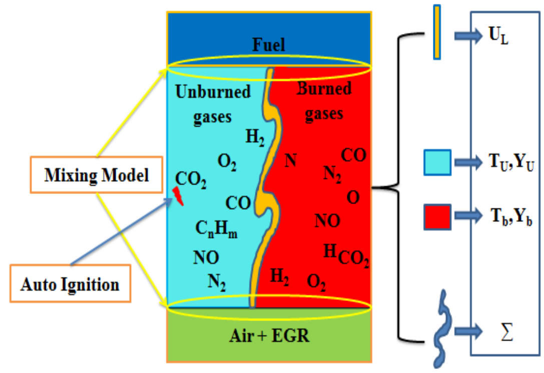

Figure 2. Schematic representation of three zones of ECFM-3Z model

For the combustion analysis of CI engine in conventional mode turbulent mixing, flame propagation, diffusion combustion models and post flame emission models were used. For HCCI mode mixing model, post flame emissions model and double delay auto ignition models were used.

For wall-bounded flows, most turbulence is generated in the near-wall region. It is therefore necessary to resolve the details of the near-wall flow, which in turn requires a fine mesh in that region. Angelberger et al., (1997), wall function model is used.

The mixed zone is the result of turbulent + molecular mixing between gases in the other two zones and is where combustion takes place.

The other two zones are characterized by the fuel in the unmixed fuel zone and the species in the unmixed air + EGR zone.

The equations governing the mass fractions of the unmixed fuel (Y_{fum}) is shown in Eq.(7):

$$\frac{\partial \rho Y_{fum}}{\partial t} + \nabla\cdot\left(\rho u Y_{fum}\right) - \nabla\cdot\left[\left(D + \frac{\mu_t}{SC_t}\right)\nabla Y_{fum}\right] = \frac{\beta_{m\,in}}{\pi} Y_{fum}\left(1 - Y_{fum}\,\frac{\rho}{\rho_u}\frac{w_m}{w_f}\right) + \dot{\omega}_e Vap \qquad (7)$$

NO_x model

The high temperatures during the combustion process facilitate the formation of nitrous oxides consisting of NO_2 and NO due to the reaction between the atmospheric nitrogen with oxygen. NO_X emissions are highly affected by the temperature. The higher the combustion temperatures the higher will be the formation of NO_x. There are two possible sources of nitrous oxide formation in engines, namely, thermal and prompt NO_x. In diesel engines, however, more than 90% of the NO emission stems from the thermal NO formation process. The current approach to modeling NO production is with the Extended Zel'dovich mechanism Pattersone et al., (1994). The Extended Zel'dovich mechanism consists of the following equations as described by Bowman (1975)

$$O + N_2 \longleftrightarrow NO + N \qquad (8)$$

$$N + O_2 \longleftrightarrow NO + O \qquad (9)$$

$$N + OH \longleftrightarrow NO + H \qquad (10)$$

With the partial equilibrium of Eq. (10) for the hydrogen radicals,

$$O + OH \longleftrightarrow O_2 + H \qquad (11)$$

The Extended Zel'dovich mechanism can be written as a single rate equation for NO, as originally put forth by Heywood (1988) is shown in Eq.(12):

$$\frac{d}{dt}[NO] = 2k_{1f}[O][N_2]\left\{\frac{\{1-[NO]^2/K_{12}[o_2]\Sigma\, d_2\}}{1+k_{1b}[NO]\Big/\left(k_{2f}[o_2]+k_{3f}[OH]\right)}\right\} \quad (12)$$

where $K_{12}=(k_{1f}/k_{1b})(k_{2f}/k_{2b})$ and the subscripts 1, 2 and 3 refer to Eqs.(8), (9) and (10), respectively. O, OH, O_2 and N_2 are assumed to be in local thermodynamic equilibrium.

Soot modeling

Soot formation is the most common process that can be observed during the combustion of fuel-rich hydrocarbons. Fuel pyrolysis and oxidation, formations of polycyclic and aromatic hydrocarbons, the inception of first particles are the complex reactions that are involved in the formation of soot. A laminar flamelet model where the scalar quantities related to scalar dissipation rates and mixture fractions developed by Karlson et al., (1998), is used to model the soot. Karlson developed a correlation between the rate of soot formation with premixed counter flow flames and local conditions in diffusion flames. In this method, an additional transport equation for the soot mass fraction is solved. Integration of mass fraction space with probability density function is taken to get the soot volume fraction source term from the flamelet library. In order to save computer storage and CPU time, the flamelet library of sources is constructed using a multi parameter fitting procedure resulting in simple algebraic and a proper set of parameters. The transport equation for soot mass fraction is shown in Eq.(13):

$$\frac{\partial}{\partial t}(\rho Y_s) + \frac{\partial}{\partial x_j}(\rho u_j Y_s) = \frac{\partial}{\partial x_j}\left(\frac{\mu_t}{Pr_{t,S}}\frac{\partial Y_s}{\partial x_j}\right) + \rho_s \bar{\omega}_v \quad (13)$$

where *Ys* is the soot fraction. The Prandtl number for soot is assumed to be 1.3 and the soot density ρ_s=1860 kg/m^3.

$$\bar{\omega}_{v,i} = \alpha_i \int_0^{\alpha}\int_0^1 \frac{1}{f_v}\left(\frac{\partial f_{v,i}}{\partial t}\left(\hat{f},\hat{\chi}\right)\right) P\left(\hat{f},\hat{\chi}\right) d\hat{f}\, d\hat{\chi} \quad (14)$$

$i = s_{g,fr,OX}$, where $\hat{\chi}$ *is* the scalar dissipation rate. In the above equation, s_g stands for surface growth, fr for fragmentation, ox for oxidation, and α_i are the scaling factors corresponding to each of these effects. They enable the user to scale the rates up or down for sensitivity studies or for calibration purposes.

INITIAL AND BOUNDARY CONDITIONS

Wall boundary conditions are used in the present analysis. The U, V components of the velocity of the inlet charge is calculated from a formula below, the Ω is taken as 2000.

$$U = -(x, -x_{CSYS})\, X\, \left(\frac{\Omega X 2\pi}{60}\right) \quad (15)$$

$$V = -(y, -y_{CSYS})\, X\, \left(\frac{\Omega X 2\pi}{60}\right) \quad (16)$$

To begin with, an absolute pressure 9.87 bar, with 0% EGR, temperature to 583 K, equivalence ratio as 0.5 are taken as initial values. Fixed boundary wall temperatures are taken with combustion dome regions as 450 K, piston crown regions as 450 K, and cylinder wall regions as 400 K. The Angleberger wall function mode is considered Moureau et al.,(2005). The 'two-layer' and low Reynolds number approaches, where no-slip conditions are applied directly and the boundary layers are computed by solving the mass, momentum and turbulence equations (the latter in their 'low Reynolds number' form) within them. The hybrid wall boundary condition which is a combination of two layered and low-Reynolds number wall boundary conditions is considered in this analysis. This hybrid wall boundary condition removes the burden of having to ensure a small enough near-wall value for y^+ (by creating a sufficiently fine mesh next to the wall). The y^+ independency of the hybrid wall condition is achieved using either an asymptotic expression valid for $0.1 < y^+ < 100$ or by blending low-Reynolds and high-Reynolds number expressions for shear stress, thermal energy and chemical species wall fluxes. This treatment provides valid boundary conditions for momentum, turbulence, energy and species variables for a wide range of near-wall mesh densities.

Hybrid wall functions are used to calculate the variables at the near wall cells and the corresponding quantities on the wall. The initial conditions were specified at IVC, consisting of a quiescent flow field at pressure and temperature for full load condition.

CFD MODEL VALIDATION

STAR-CD is a well known Commercial CFD package and is well validated. The validation of the package with the experimental results was done by many authors like Pasupathy Venkateswaran *et* al.,(2010), Zellat Marc et al., (2005), Bakhshan, et al., (2011), A comparison of the CI engine in HCCI and conventional modes are done in this paper considering the extended coherent flame combustion three zones, a compression model for combustion analysis.

RESULTS AND DISCUSSION

In the present study the experimental study of D. Ganesh et al., (2008), on a single cylinder HCCI engine was simulated, using a three-zone extended coherent flame (ECFM-3Z) CFD model. The computational and experimental results (emissions and combustion characteristics) of diesel HCCI combustion (external mixture formation) with various EGR proportions were compared.

Oxides of nitrogen emissions

In the following EDVI represents Experimental Diesel vapor Induction, SDVI represents Simulated Diesel vapor induction, EDDI represents Experimental Direct Diesel Injection condition, and SDDI represents Simulated Direct Diesel Injection condition. The % EGR representation beside each notation represents the % of EGR used. NO in IC engine will form in hot zones whereas the soot forms in fuel rich zones. If the fuel and air were mixed before combustion there is a chance to reduce the PM and NO_x emissions by maintaining lean air/fuel ratios globally.

A Fuel vaporizer was used in the present study to form homogeneous mixture of air and fuel. The vaporizer is connected to the intake manifold to form the HCCI combustion. NOx emissions reduction up to 90-95% is possible with the HCCI combustion, and further reduction is possible by using cold EGR which acts as a heat sink in avoiding hot zones in the combustion zones because of the thermal effect of CO_2 in absorbing the heat.

The aim of this study is to reduce exhaust raw emission of NOx and smoke by homogenization of the combustion. This is achieved by using an appropriate diesel fuel premixing technology i.e. external mixing of diesel fuel and air.

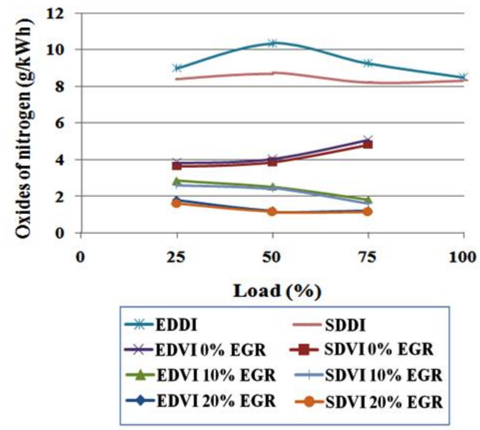

Figure 3. Variation of oxides of nitrogen with load

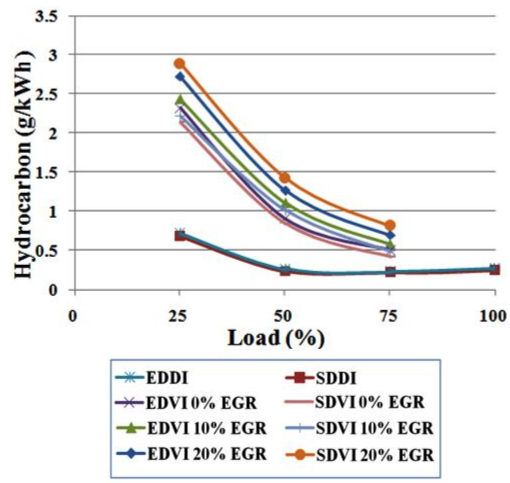

Figure 4. Variation of hydrocarbon with load

Figure 3. shows the results of both experimental and simulation of the variation of oxides of nitrogen with load for diesel vapor induction with 0%, 10%, and 20%, EGR. The figure clearly shows that the NOx emission reduces by 45%, 80%, 86% and 95% respectively for diesel vapor induction with 0%, 10%, and 20%, EGR at 75% load condition compared with that of the conventional diesel combustion. The ECFM -3Z compression ignition model simulation results are in good agreement with the experimental results. But a slightly lower NO_x are recorded in case of simulation results when compared to the experimental results. This is because of the adiabatic conditions assumed in the simulation process.

Hydrocarbon emissions

The major drawback of HCCI engines are their higher HC and CO emissions because of the low temperature combustion due to lean charge and higher EGR. Low temperatures in HCCI combustion inhibit the oxidation of the HC. Fig. 4 shows the experimental and simulation results of variation of hydrocarbon emission with load. In HCCI mode, the HC and CO emissions are typically around 30 times higher than the standard diesel operation Megaritis et al., (2007), Juttu et al., (2007), Odaka Matsuoet al.,(1999), Jacobs Timothy et al., (2007), Miller et al.,(2008) and Lu¨ Xing-cai et al.,(2005). The hydrocarbon emissions are 0.51 g/kWh, 0.59 g/kWh, 0.69 g/kWh and 0.81 g/kWh at 75% load condition for diesel vapor induction with 0%,10%, 20%, and 30% EGR whereas in conventional diesel operation it is about 0.25 g/kWh. The simulation results are in good agreement with the experimental results. Lower HC values are recorded in the simulation results when compared with the experimental results. The reason behind it is the oxidation of the HC as the wall temperatures of the combustion chamber are not mapped, but are fixed in the simulation, to reduce the computational time.

Carbon monoxide emissions:

The combustion reaction rate reduces with increase in EGR. With the increase in EGR in-cylinder temperatures decrease causing combustion to be more incomplete, because the CO is not completely oxidized to CO_2 at low temperatures. Fig. 5 shows the experimental and simulation results for variation of carbon monoxide emission with load. The carbon monoxide emissions are 4.32 g/kWh, 5.06 g/kWh, 6.3 g/kWh and 7.5 g/kWh at 75% load for diesel vapor induction with 0%, 10%, 20%, and 30% EGR whereas in conventional diesel operation it is about 1.28 g/kWh. The simulation results are slightly higher than the experimental results. The reason is because over prediction of the CO values and the input values considered for calculating the CO emissions. The HCCI combustion achieved by a lean mixture of charge and high EGR are responsible for the increase in HC and CO emissions mitigating the oxidation reactions at low temperatures.

In-cylinder pressure

The simulated results of variation of in-cylinder pressure (in bar) with crank angle (in degrees) at EGR proportions of 0%, 10% and 20% are shown in the Fig. 6 in diesel vapor induction HCCI mode. The peak pressures at 20% EGR are lower in comparison with the 0% and 10% EGR which are almost same.

The reason for a decrease in in-cylinder pressure at 20% EGR is due increased heat absorption capacity of CO_2 in the EGR used Morsy Mohamed H (2007). It is also observed that with increase in EGR the peak cylinder pressure occurs before and close to TDC.

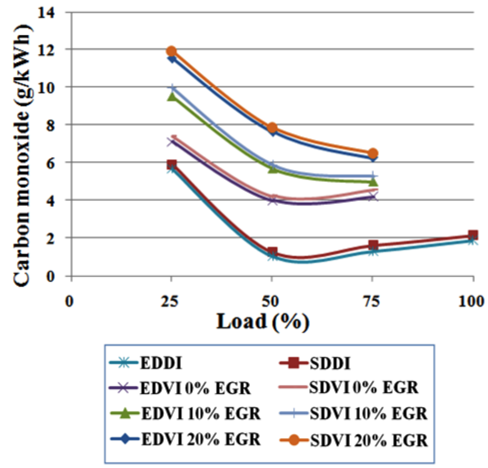

Figure 5. Variation of carbon monoxide with load

Turbulent kinetic energy

Turbulent kinetic energy is an important parameter to determine the burn time and flame speed at a particular region Yongxian et al., (2006). The turbulence controls the flow dissipation rate, flame propagation rate and heat transfer and it is quantified by the turbulent kinetic energy within the cylinder. The regions with low turbulent kinetic energy represents the relatively long time for these parts of the flame front to disappear.

Turbulent kinetic energy depends on the kinematic viscosity. The kinetic energy of the incoming flow contributes to the turbulent kinetic energy within the cylinder. Fig. 7 shows the contour plots of turbulent kinetic energy at 740 CA and at different EGR concentrations. A clear variation in turbulent kinetic energy was observed with the increase in EGR concentration due to the heat absorption capability of CO_2 in EGR.

Velocity magnitude

Velocity magnitude of the combustion chamber gives us a clear idea about the efficient combustion in the combustion chamber. Fig. 8 shows the contour plots velocity magnitude at 740 CA and at different EGR concentrations. Velocity magnitude of combustion chamber gives the better idea to locate the regions where the incomplete combustion occurs and to be improved. The poor velocity regions in the combustion volume represent the poor mixing of the fuel and air leading to incomplete combustion. This shows the need for better combustion chamber designs to create proper turbulence to for the better mixture formation.

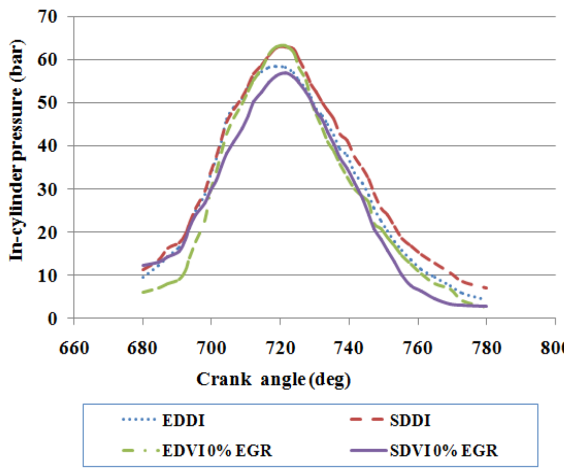

(a)

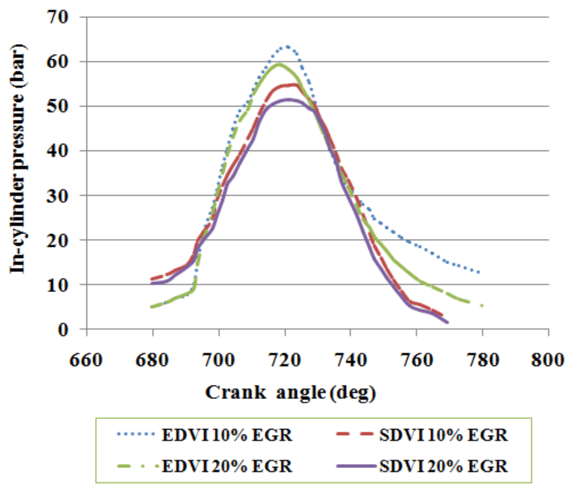

(b)

Figure 6. Variation of In-cylinder pressure with crank angle at different EGR concentrations

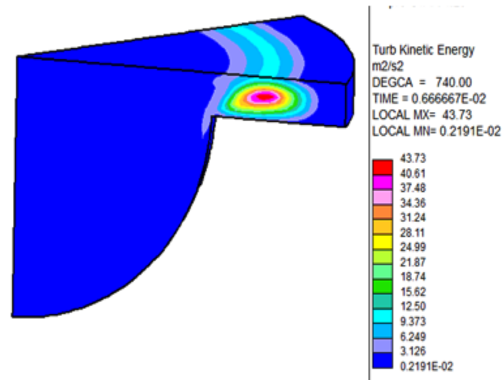

(a) 0% EGR

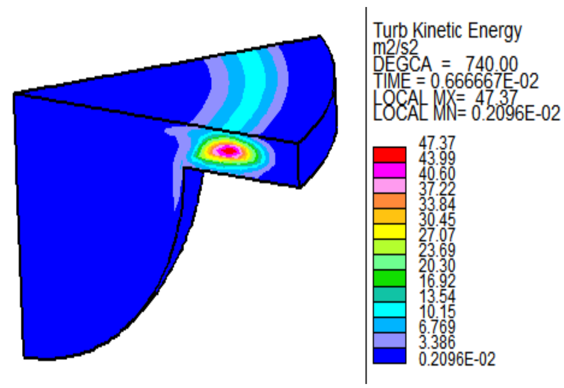

(b) 10% EGR

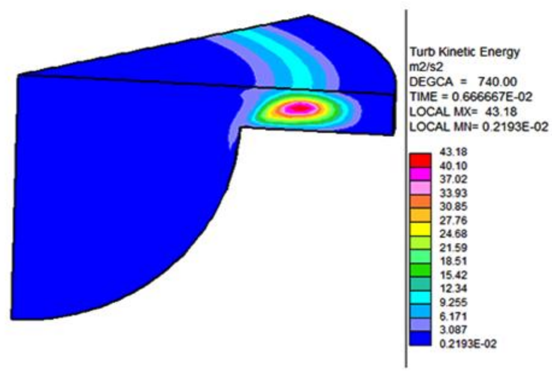

(c) 20% EGR

Figure 7. Variation of Turbulent Kinetic Energy with EGR Concentration

Apparent Heat Release:

Apparent heat release is one of the important engine parameters to study the combustion process occurring in the cylinder. It provides information about at which point of combustion the maximum heat is getting released and also gives information about combustion stages. Fig.9 shows the simulated results of the apparent heat release at different EGR concentrations.

From Fig. 9 it is clear that the peak apparent heat release increased a slightly with the addition of 10% EGR (186 J/deg CA) when compared to 0% EGR (178.5 J/deg CA), and then decreased by further addition of EGR i.e. 20% EGR (164 J/deg CA). At 0% EGR cool flame auto-ignition occurs prior main auto-ignition, releasing a small quantity of heat. At 10% EGR this cool flame auto-ignition was not observed. This due to the higher initial temperatures suitable for main auto-ignition with increased EGR concentration.

This results in higher apparent heat release and earlier auto-ignition at early crank angles. In case of 20% EGR instead of increasing the initial temperatures the CO_2 present in the EGR absorbed the heat so the auto ignition is delayed and peak apparent heat release is decreased.

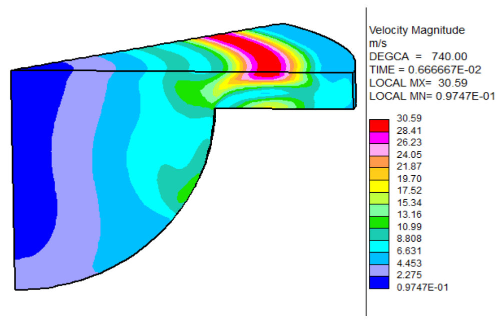

(a) 0% EGR

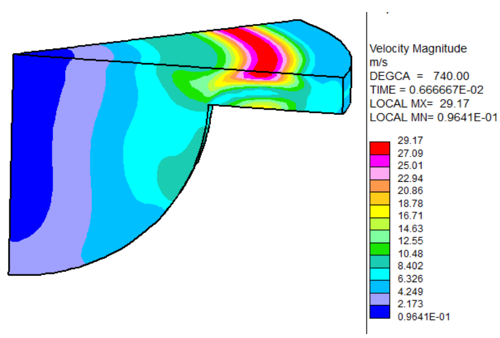

(b) 10% EGR

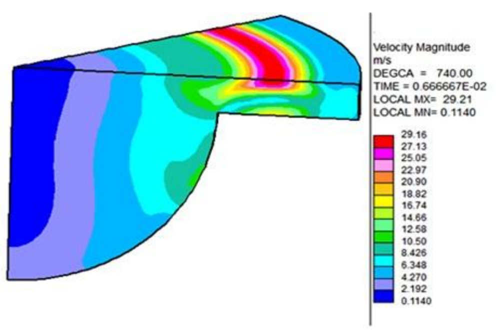

(c) 20% EGR

Figure 8. Variation of Velocity Magnitude with EGR concentration

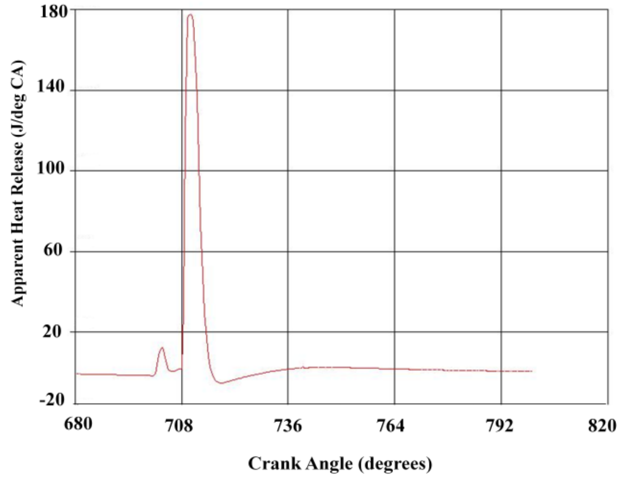

(a) 0% EGR

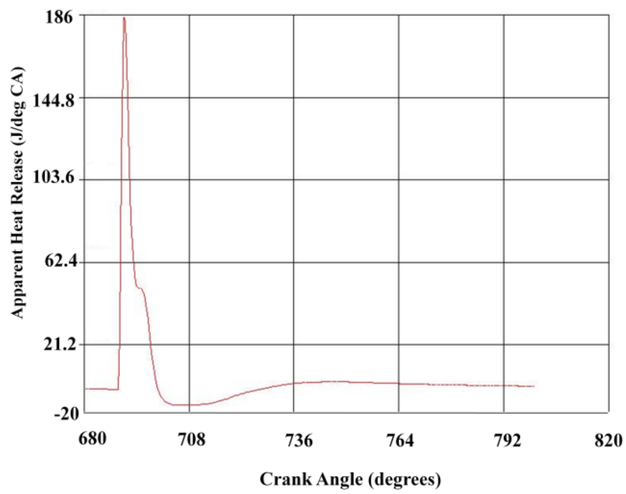

(b) 10% EGR

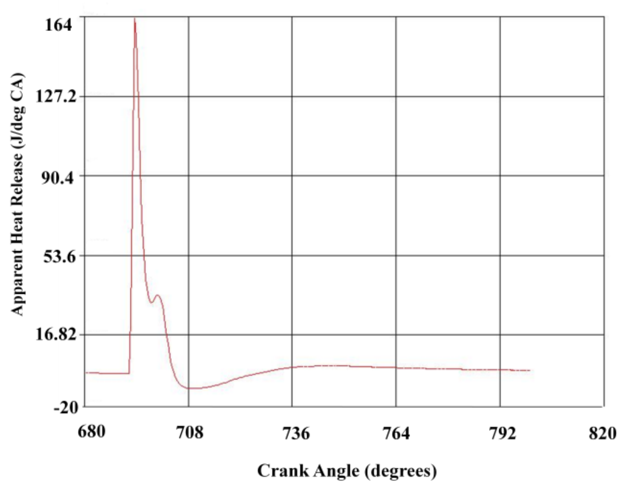

(c) 20% EGR

Figure 9. Variation in Apparent Heat Release with EGR Concentration

Piston work:

Figure 10. shows the variation of piston work with EGR concentration. There is a decrease in piston with increase in EGR concentration. This is because of the reduction in in-cylinder temperatures with EGR. As EGR is mainly intended to reduce the combustion temperatures to reduce the NO_x emissions, the work done by the piston is getting scarified due to reduced combustion temperatures.
Though the piston work is reduced by 10% EGR it increases slightly by the 20% EGR due to the improved heat at the beginning of the combustion process.

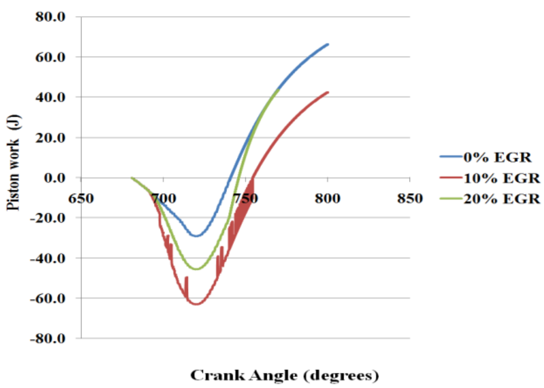

Figure 10. Variation of piston work with EGR concentration

CONCLUSIONS

3D CFD simulations of a HCCI diesel engine with external mixture formation have been carried out to investigate the effect of EGR on the engine performance and combustion efficiency at different load conditions. Three different EGR concentrations of 0%, 10% and 20% are studied with respect to in-cylinder pressure, performance and emissions. Comparison of experimental results of the engine has been done using Extended Coherent Flame combustion analysis considering three zones. The model used was validated by many authors. The present analysis revealed many issues emphasizing problems associated with complete combustion with increase in EGR concentration and at the same time it also revealed the limitation of the HCCI mode of combustion and the necessary issues to be addressed to overcome the same. The contour plots of turbulent kinetic energy and velocity magnitudes revealed more uniform distribution of fuel-air mixture in HCCI mode at different EGR concentrations.

Acknowledgements

The authors would like to thank Dr.Raja Banerjee Associate Professor from IIT Hyderabad for allowing us to use computational facility at IITH, Mr.B.Siva Nageswara Rao from CD-adapco for his support and Mr.P.Madhu computer lab incharge IITH for his support during the simulation work.

REFERENCES

Epping, K., Aceves, S. M., Bechtold, R. L., and Dec, J. E., 2002, "The Potential of HCCI Combustion for High Efficiency and Low Emissions," *SAE Paper No. 2002-01-1923.*

Thring RH., 1989. "Homogeneous-charge compression ignition (HCCI) engines," *SAE Paper No 892068. Warrendale, PA: Society of Automotive Engineers Inc.*

Yanagihara H., 2001. "Ignition timing control at Toyota ''unibus'' combustion system. A new generation of engine combustion processes for the future," *In: Proceedings of the IFP international congress; p. 34–42.*

Shi Lei, Cui Yi, Peng Kangyao, chen Yuanyuan., 2006. "Study of low emission homogeneous charge compression ignition (HCCI) engine using combined internal and external exhaust gas recirculation (EGR)," *Energy;31:2665–76.*

Simescu Stefan, Fiveland Scott B, Dodge Lee G., 2003. "An experimental investigation of PCCI-DI combustion and emissions in a heavy-duty diesel engine," *SAE paper no 2003-01-0345.*

Midlam-Mohler Shawn, Guezennec Yann, Rizzoni Giorgio., 2003. "Mixed-mode diesel HCCI with external mixture formation," *DEER 2003 Newport; August 26th.*

Duclos, J.M., Zolver, M.,Baritaud., 1999. "3D modeling of combustion for DI-SI engines," *Oil & Gas Science and Technology – Rev. IFP*, 54(2), pp. 259-264.

Colin, O. and Benkenida., A. 2004. "The 3-Zone Extended Coherent Flame Model (ECFM3Z) for computing premixed/diffusion combustion," *Oil & Gas Science and Technology – Rev. IFP*, 59(6), pp. 593-609.

Ravet, F., Abouri, D., .Zellat, M.,Duranti, S., 2008, "Advances in Combustion Modeling in STAR-CD: Validation of ECFM CLE-H Model to Engine Analysis," *18th Int. Multidimensional Engine Users' Meeting at the SAE Congress - April, 13 2008, Detroit.*

Subramanian, G.,Vervish, L. and Ravet, F., 2007, "New Developments in Turbulent Combustion

Modeling for Engine Design: ECFM-CLEH Combustion Submodel," *SAE International - 2007-01-0154.*

Huh, K.Y., and Gosman., A.D. 1991. "A phenomenological model of Diesel spray atomization," *Proc. Int. Conf. on Multiphase Flows (ICMF '91), Tsukuba, 24-27 September.*

Bai, C., and Gosman,A.D., 1995, "Development of Methodology for Spray Impingement Simulation," *SAE Technical Paper Series, SAE Paper No. 950283.*

Reitz, R. D., and Diwakar,R., 1987, "Structure of High-Pressure Fuel Spray," *SAE Technical Paper Series, SAE Paper No. 870598.*

Reitz, R. D., and Diwakar,R., 1986, "Effect of Drop Breakup on Fuel Sprays," *SAE Technical Paper Series, SAE Paper No. 860649.*

Angelberger,C.,Poinsot,T., and Delhay, B. 1997. "Improving Near-Wall Combustion and Wall Heat Transfer Modeling in SI Engine Computations," *SAE Technical Paper Series 972881, pp. 113-130*.

Patterson, M. A., Kong, S. -C., Hampson, G. J., Reitz,R.D., *1994.*"Modeling the Effects of Fuel Injection Characteristics on Diesel Engine Soot and NOx Emissions," *SAE Paper 940523*.

Bowman, C. T., 1975. "Kinetics of Pollutant Formation, Destruction in Combustion," *Prog. Energy Combust. Sci.,* **1**, 33.

Heywood, J. B., 1988. "Internal Combustion Engine Fundamentals," *McGraw-Hill Company.*

Karlsson, A., Magnusson, I., Balthasar, M., Mauss,F., 1998, "Simulation of Soot Formation Under Diesel Engine Conditions Using a Detailed Kinetic Soot Model," *SAE Technical Paper Series, SAE Paper No. 981022.*

V. Moureau, G. Lartigue, Y. Sommerer, C. Angelberger, O. Colin,T. Poinsot., 2002. "Numerical Methods for Unsteady Compressible Multi-Component Reacting Flows on Fixed and Moving Grids," *In. Journal of Computational Physics, 202-2:710-736, 2005.*

Pasupathy Venkateswaran, S., G. Nagarajan., 2010. "Effects of the Re-Entrant Bowl Geometry on a DI Turbocharged Diesel Engine Performance and Emissions—A CFD Approach," *Journal of engineering for gas turbines and power* 132.12.

Zellat, Marc, et al., 2005. "Towards a universal combustion model in STAR-CD for IC engines: from GDI to HCCI and application to DI Diesel combustion optimization," *Proc. 14th Int. Multidimensional Engine User's Meeting, SAE Cong*.

Y.Bakhshan, et al., 2011. "Multi-Dimensional Simulation of n-Heptane Combustion under HCCI Engine Condition Using Detailed Chemical Kinetics," *The Journal of Engine Research/Vol. 22 / Spring.*

Ganesh, D., G. Nagarajan, M. Mohamed Ibrahim., 2008. "Study of performance, combustion and emission characteristics of diesel homogeneous charge compression ignition (HCCI) combustion with external mixture formation," *Fuel*87.17 (2008): 3497-3503.

Megaritis A, Yap D, Wyszynski ML., 2007. "Effect of water blending on bioethanol HCCI combustion with forced induction and residual gas trapping," *Energy;32:2396–400.*

Juttu S, Thipse S, Marathe NV, Gajendra Babu MK., 2007. "Homogeneous charge compression ignition (HCCI): a new concept for near zero NOx and particulate matter (PM) from diesel engine combustion," *SAE paper no 2007-26-020*.

Odaka Matsuo, Suzuki Hisakazu, Koike Noriyuki, Ishii Hajime., 1999. "Search for optimizing control method of homogeneous charge diesel combustion," *SAE paper no 1999-01-0184*.

Jacobs Timothy J, Assanis Dennis N., 2007. "The attainment of premixed compression ignition low-temperature combustion in a compression ignition direct injection engine," *In: Proc. of the combustion institute, vol. 31. p. 2913–20.*

Miller Jothi NK, Nagarajan G, Renganarayanan S., 2008. "LPG fueled diesel engine using diethyl ether with exhaust gas recirculation," *International Journal of Thermal Sciences;47:450–7.*

Lu¨ Xing-cai, Chen Wei, Hou Yu-chun, Huang Zhen., 2005. "Study on ignition, combustion and emissions of HCCI combustion engines fueled with primary reference fuels," *SAE paper no 2005-01-0155.*

Morsy Mohamed H., 2007. " Ignition control of methane fueled homogeneous charge compression ignition engines using additives," *Fuel ;86:533–40.*

Yongxian, Gu, J. R. Mayor, and W. J. A. Dahm., 2006. "Turbulence - augmented minimization of combustion time in mesoscale internal combustion engines," *44th AIAA aerospace sciences meeting and exhibit, AIAA-2006-1350.*